

Article

Synthesis of DHA/EPA Ethyl Esters via Lipase-Catalyzed Acidolysis Using Novozym[®] 435: A Kinetic Study

Chia-Hung Kuo ^{1,*}, Chun-Yung Huang ¹, Chien-Liang Lee ², Wen-Cheng Kuo ³,
Shu-Ling Hsieh ¹ and Chwen-Jen Shieh ^{4,*}

¹ Department of Seafood Science, National Kaohsiung University of Science and Technology, Kaohsiung 811, Taiwan; cyhuang@nkust.edu.tw (C.-Y.H.); slhsieh@nkust.edu.tw (S.-L.H.)

² Department of Chemical and Materials Engineering, National Kaohsiung University of Science and Technology, Kaohsiung 807, Taiwan; cl_lee@nkust.edu.tw

³ Department of Mechatronics Engineering, National Kaohsiung University of Science and Technology, Kaohsiung 811, Taiwan; rkuo@nkust.edu.tw

⁴ Biotechnology Center, National Chung Hsing University, Taichung 402, Taiwan

* Correspondence: kuocho@nkust.edu.tw (C.-H.K.); cjshieh@nchu.edu.tw (C.-J.S.);
Tel.: +886-7-361-7141 (ext. 23464) (C.-H.K.); +886-4-2284-0450 (ext. 5121) (C.-J.S.)

Received: 14 April 2020; Accepted: 12 May 2020; Published: 19 May 2020



Abstract: DHA/EPA ethyl ester is mainly used in the treatment of arteriosclerosis and hyperlipidemia. In this study, DHA+EPA ethyl ester was synthesized via lipase-catalyzed acidolysis of ethyl acetate (EA) with DHA+EPA concentrate in *n*-hexane using Novozym[®] 435. The DHA+EPA concentrate (in free fatty acid form), contained 54.4% DHA and 16.8% EPA, was used as raw material. A central composite design combined with response surface methodology (RSM) was used to evaluate the relationship between substrate concentrations and initial rate of DHA+EPA ethyl ester production. The results indicated that the reaction followed the ordered mechanism and as such, the ordered mechanism model was used to estimate the maximum reaction rate (V_{max}) and kinetic constants. The ordered mechanism model was also combined with the batch reaction equation to simulate and predict the conversion of DHA+EPA ethyl ester in lipase-catalyzed acidolysis. The integral equation showed a good predictive relationship between the simulated and experimental results. 88–94% conversion yields were obtained from 100–400 mM DHA+EPA concentrate at a constant enzyme activity of 200 U, substrate ratio of 1:1 (DHA+EPA: EA), and reaction time of 300 min.

Keywords: lipase; acidolysis; docosahexaenoic acid ethyl ester; eicosapentaenoic acid ethyl ester; ethyl acetate; kinetics

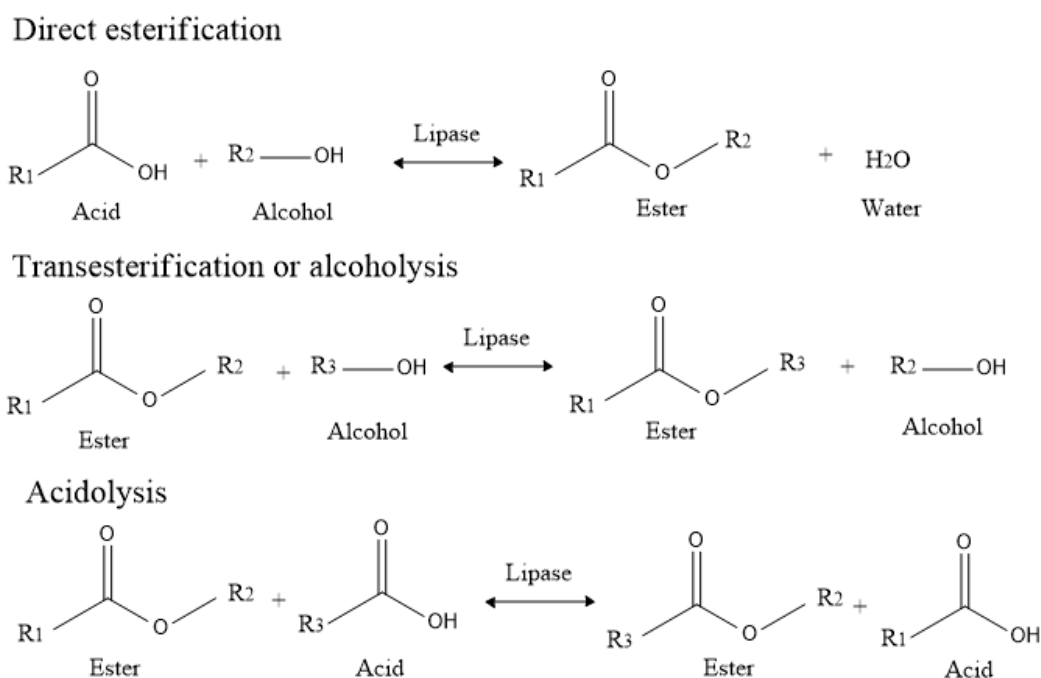
1. Introduction

Docosahexaenoic acid (DHA; C22:6) and eicosapentaenoic acid (EPA; C22:6) belong to *n*-3 polyunsaturated fatty acids (PUFAs) have unique physiological activities and health functions, are considered essential fatty acids. Thanks to increasing health concerns, the fish oil market has expanded and the amount of fish oil used in health products is growing rapidly. In 2014, the consumption of fish oil was about 282,000 tons with a market value of more than 1.69 billion USD [1]. Fish oils are rich in long-chain *n*-3 PUFAs, especially DHA and EPA [2]. The health benefits of DHA and EPA have been widely investigated, including their impact on cardiovascular disease [3,4], ethanol-induced fatty liver [5], blood pressure [6], asthma [7], and inflammation [8]. With advancements in industrial technology and the widespread use of biochemical technology, the concentration and purity of DHA and EPA are increasing in food products and medicinal grade drugs [8]. Generally, the DHA

and EPA content in fish oil is less than 30% [9]. For health products or medicinal applications, fish oil must use physical, chemical, or enzymatic methods to concentrate n-3 PUFAs. Various concentration methods have been reported, including low temperature solvent crystallization [10], urea complexation [11,12], molecular distillation [13], supercritical fluid extraction [14], high-performance liquid chromatography [15], silver nitrate extraction [16], solvent fractionation [17], and enzymatic methods [18–20]. However, concentrated n-3 PUFAs are unstable and difficult to preserve for long periods due to the carboxyl groups enhanced the catalytic effect to form the free radicals by the decomposition of hydroperoxides [21], and therefore must be esterified as triglycerides or ethyl esters to increase storage stability.

Generally, chemical esterification employs a strong acid, alkaline, or metal (Lewis acid) as the chemical catalyst. These catalysts have several problems, such as reaction at a higher temperature (>160 °C), unwanted side reactions that cause darkening or odors, or the product poses environmental threats [22]. An alternative to chemical-based esterification, biocatalysis seems to be an attractive option for producing esters. Lipase (triacylglycerol ester hydrolase, EC 3.1.1.3) hydrolyses ester linkages of triglycerides into glycerol and fatty acids [23,24]. On the other hands, the lipase catalyzes the reverse synthesis reaction to produce esters in the non-aqueous organic system [25,26]. Immobilized lipase is typically used in this reaction since immobilization improves the life and stability of the enzyme, as well as facilitating enzyme recovery, reuse, and continuous operation [27,28]. Immobilization of lipase may alter its observed activity, specificity or selectivity [29]. Lipases exist in two main forms, open and closed forms [30]. The hydrophobic supports fix the structure of lipase at the open conformation [31], which can promote hyperactivation of lipase after immobilization [32–34]. Novozym[®] 435 is a commercially available immobilized lipase produced by Novozymes. It is based on immobilization via interfacial activation of lipase B from *Candida antarctica* on a macroporous support formed by poly(methyl methacrylate) crosslinked with divinylbenzene, which has been used for synthesis of many esters [35]. Shimada et al. used immobilized lipase from *Candida antarctica* to catalyze DHA and ethanol for the synthesis of DHA ethyl ester; a high yield of 88% was obtained after 24 h [36]. DHA ethyl ester has been synthesized by both lipase-catalyzed transesterification of lipids with ethanol and lipase-catalyzed esterification of fatty acids with ethanol, with conversion yields of 20% and 60% after 24 h, respectively [37]. Bhandari et al. used immobilized lipase from *Candida antarctica* for the esterification of glycerol with n-3 PUFA, and a high degree of esterification (69%) was obtained after 24 h [38]. However, the reaction normally requires a reaction time of around 24 h.

Lipase catalyzed synthesis of ester can be achieved in different ways [39], as depicted in Scheme 1. This process normally takes place between an acid and an alcohol (direct esterification) [40,41], an ester and an alcohol (transesterification or alcoholysis) [42], an ester and an acid (acidolysis) [43], or between two esters (interesterification) [44]. Our previous research determined that ester synthesized by lipase via transesterification (alcoholysis) exhibited higher reaction rates than that obtained via direct esterification [41,42]. In this study, in order to decrease reaction time and increase the conversion yield, we chose ethyl acetate as the ester for the lipase-catalyzed synthesis of DHA+EPA ethyl esters via acidolysis with DHA+EPA concentrate. Lipase-catalyzed acidolysis has been used to incorporate citronellic acid and myristic acid into egg-yolk phosphatidylcholine [45,46], and to incorporate caprylic acid into corn oil for the synthesis of MLM structured lipids [47], but to date, the lipase-catalyzed synthesis of DHA+EPA ethyl esters via acidolysis of EA with DHA+EPA concentrate has not been reported.



Scheme 1. Lipase-catalyzed synthesis of ester via direct esterification, alcoholysis or acidolysis.

It is useful to know the reaction kinetics and the constants that describe kinetic behavior of the reaction. The ping-pong bi-bi mechanism or an ordered bi-bi mechanism is the most used kinetic models for explaining the reaction of lipase-catalyzed esterification or transesterification [48]. Lipase-catalyzed reactions with free or immobilized enzymes and with substrates (acids and alcohols) of various chain lengths and structures, either in solvent-free systems or in the presence of an organic solvent have been carried out for kinetic studies [49–51]. However, the kinetics and modelling of lipase-catalyzed acidolysis of EA with concentrated n-3 PUFAs have not yet been discussed. The aim of this research was to investigate the kinetics of lipase-catalyzed synthesis of DHA+EPA ethyl esters via acidolysis in order to identify the optimal conditions for ester synthesis. In this study, a statistical experimental design and response surface methodology (RSM) analysis were employed to investigate the kinetic model for determining kinetic constants. Finally, a kinetic model based on the estimated kinetic constants was developed and used for predicting conversion yields of lipase-catalyzed acidolysis in batch reactions.

2. Results and Discussion

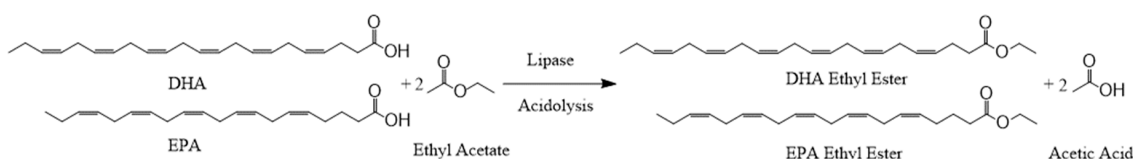
2.1. Initial Rate of DHA+EPA Ethyl Ester Production

In order to understand the lipase-catalyzed acidolysis reaction for DHA+EPA ethyl ester synthesis, analysis of the reaction kinetics and the constants is useful to describe the reaction mechanism. In general, the initial rate data were fitted to the proposed kinetic model in order to evaluate the kinetic constants. Therefore, a great number of the initial rate data performed through a wide range of substrate concentrations are required to measurement from systematic experiments. A more efficient technique to solve the problem is response surface methodology (RSM), which can be used for obtaining sufficient data to solve the kinetic parameters under the less number of experimental runs and time. The lipase-catalyzed acidolysis of EA with DHA+EPA concentrate is represented in Scheme 2. With the purpose of finding a kinetic model to illustrate the relationship between the DHA+EPA concentrate and EA in the reaction, the effect of substrate concentrations on the initial rate of DHA+EPA ethyl ester production was investigated. A five-level-two-factor central composite design was employed and combined with RSM in order to better understand the relationship between substrate concentration

and initial production rate. The DHA+EPA concentrate prepared by using the acetone fractionation of fatty acid salts method [52], contained 54.4% DHA and 16.8% EPA, was used as raw material for the lipase-catalyzed synthesis of DHA+EPA ethyl ester. The substrate concentrations and their selected levels are listed in Table 1. The SAS statistical software (SAS Institute, Cary, NC, USA) was used to fit the initial rate data in Table 1 to the second-order polynomial equation. The second-order polynomial Equation (1) is as below:

$$Y (\mu\text{mol min}^{-1} \text{U}^{-1}) = -0.011807 + 0.0002X_1 + 0.000265X_2 - 0.000000451X_1X_1 + 0.000000665X_2X_1 - 0.000000757X_2X_2 \quad (1)$$

where Y is the initial rate of DHA+EPA ethyl ester production, and X_1 , and X_2 are uncoded values for DHA+EPA concentrate and EA concentration, respectively.



Scheme 2. Lipase-catalyzed synthesis of DHA+EPA ethyl ester via acidolysis of EA with DHA+EPA concentrate.

Table 1. Central composite design and initial experimental rate of DHA+EPA ethyl ester production.

Treatment No. ¹	Factor		Initial Rate of DHA+EPA Ethyl Ester Production ($\mu\text{mol min}^{-1} \text{U}^{-1} \text{Enzyme}$)
	X_1 DHA+EPA (mM)	X_2 Ethyl Acetate (mM)	
1	-2 ² (40)	0 (220)	0.0168 ± 0.0001
2	-1 (130)	-1 (130)	0.0421 ± 0.0032
3	-1 (130)	1 (310)	0.0533 ± 0.0029
4	0 (220)	-2 (40)	0.0291 ± 0.0011
5	0 (220)	0 (220)	0.0627 ± 0.0023
6	0 (220)	0 (220)	0.0639 ± 0.0020
7	0 (220)	2 (400)	0.0494 ± 0.0050
8	1 (310)	-1 (130)	0.0466 ± 0.0041
9	1 (310)	1 (310)	0.0793 ± 0.0054
10	2 (400)	0 (220)	0.0816 ± 0.0027

¹ The treatments were run in a random order; ² The values -2, -1, 0, 1, and 2 are coded levels.

The determination coefficient of 0.92 in the analysis of variance (ANOVA) data (Table 2) showed that the second-order polynomial model was fitted well to represent the actual relationship between the initial rate of DHA+EPA ethyl ester production and the substrate concentrations. The ANOVA results revealed the fitted model (Equation 1) was significant as the *p*-value was smaller than 0.05 (*p* = 0.0248). Therefore, this model was adequate for predicting the initial rate within the range of variables employed. The ANOVA results indicated that the quadratic and cross-product terms had less influence (*p* > 0.05) as compared to the linear term had a significant (*p* < 0.05) influence on the initial rate of DHA+EPA ethyl ester production.

The relationship between substrate concentration and initial rate can be better understood by analyzing the contour plot. The effects of the concentrations of both DHA+EPA concentrate and EA on the initial rate of DHA+EPA ethyl ester production is shown in Figure 1. At any given concentration of DHA+EPA, an increase in EA concentration led to an increase in the initial rate. At any given concentration of EA, the increase in concentration of DHA+EPA concentrate led to an increase in the initial rate. However, an inhibitory effect on the initial rate was seen at high concentrations of DHA+EPA concentrate (>300 mM) when EA concentration was low (50 mM). The inhibitory effect on the initial rate might cause by the high concentrations of acid substrate inhibited the lipase activity

or due to mass transfer diffusional limitations. Inhibition by high concentrations of acid substrate has been reported for lipase-catalyzed esterification of ethyl oleate [53], propyl caprate [54], isoamyl butyrate [55], and 2-ethylhexyl-2-ethylhexanoate [56].

Table 2. ANOVA for substrate concentration pertaining to the response (initial rate).

Factor ¹	Degree of Freedom	Sum of Squares	Prob > F
Model	5	0.003478	0.0248 *
Linear term	2	0.002728	0.0096 *
Quadratic	2	0.000634	0.1011
Cross-product	1	0.000116	0.2787

$R^2 = 0.92$

¹ Independent variable X_1 : DHA+EPA concentration, X_2 : EA concentration; * Significant at p -Value < 0.05

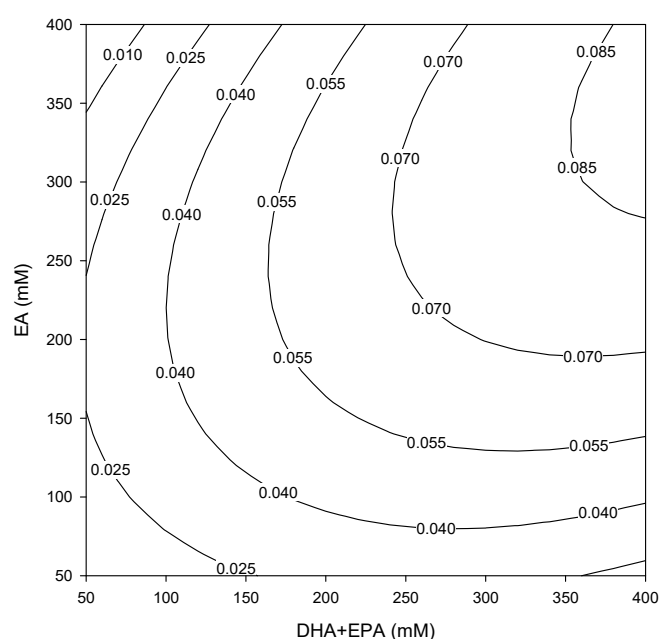


Figure 1. Contour plot showing the initial rate of DHA+EPA ethyl ester production at varying concentrations of DHA+EPA (mM) and EA (mM). Numbers on contours denote initial rate ($\mu\text{mol min}^{-1} \text{U}^{-1}$) under given reaction conditions.

2.2. Kinetic Modeling

Enzyme-catalyzed ester synthesis is usually a two-substrate reaction. The mechanism of this type of reaction is a very broad and extremely complex topic, but the mechanism by which the enzyme reacts with the substrate is crucial to the analysis of enzyme kinetics. Multi-substrate enzyme reactions can mainly be explained by three mechanisms: ping-pong bi-bi mechanism, ordered mechanism, and random-order mechanism. The first mechanism is releasing one or more products before all substrates bind with enzymes. This mechanism is a non-sequential reaction. In the other two mechanisms, the substrates must all be combined with the enzyme before the product releases. The order of substrate binding is random for the random-order mechanism, but substrates must bind in a particular sequence for the ordered mechanism. The ordered and random-order mechanisms are sequential reactions involving the formation of a ternary complex (one involving the enzyme and both substrates). The general rate equation of a two-substrate enzyme-catalyzed reaction, as derived by Alberty [57], is as follows:

$$v = \frac{V_{max}[A][B]}{K_{dA}K_{mB} + K_{mB}[A] + K_{mA}[B] + [A][B]} \quad (2)$$

where v is the initial reaction rate, V_{max} is the maximum initial reaction rate, $[A]$ is the initial concentration of DHA+EPA concentrate, $[B]$ is the initial concentration of EA, and K_{mA} and K_{mB} are the Michaelis constants for DHA+EPA and EA, respectively. K_{dA} is the dissociation constant of the DHA+EPA-lipase complex.

The reaction mechanism can be examined from the Lineweaver-Burk plot, which plots $1/v$ against $1/[A]$ at constant $[B]$. The general rate equation for reactions using a ping-pong bi-bi mechanism is simpler, in that the term of $K_{dA}K_{mB}$ is zero. The slope of the Lineweaver-Burk plot is independent of $[B]$. A series of Lineweaver-Burk plots obtained at different $[B]$ values would thus be parallel for the ping-pong bi-bi mechanism. In contrast, a series of Lineweaver-Burk plots for ordered and random-order mechanisms at different $[B]$ values showed changes in both the intercept and slope. From the RSM results, reciprocal initial reaction rates ($1/v$) were plotted against the inverse concentration of DHA+EPA concentrate ($1/[A]$) at different EA concentrations $[B]$. The Lineweaver-Burk plot in Figure 2 shows that both the intercept and slope changed at different EA concentrations. Therefore, this reaction followed either the ordered or random-order mechanism.

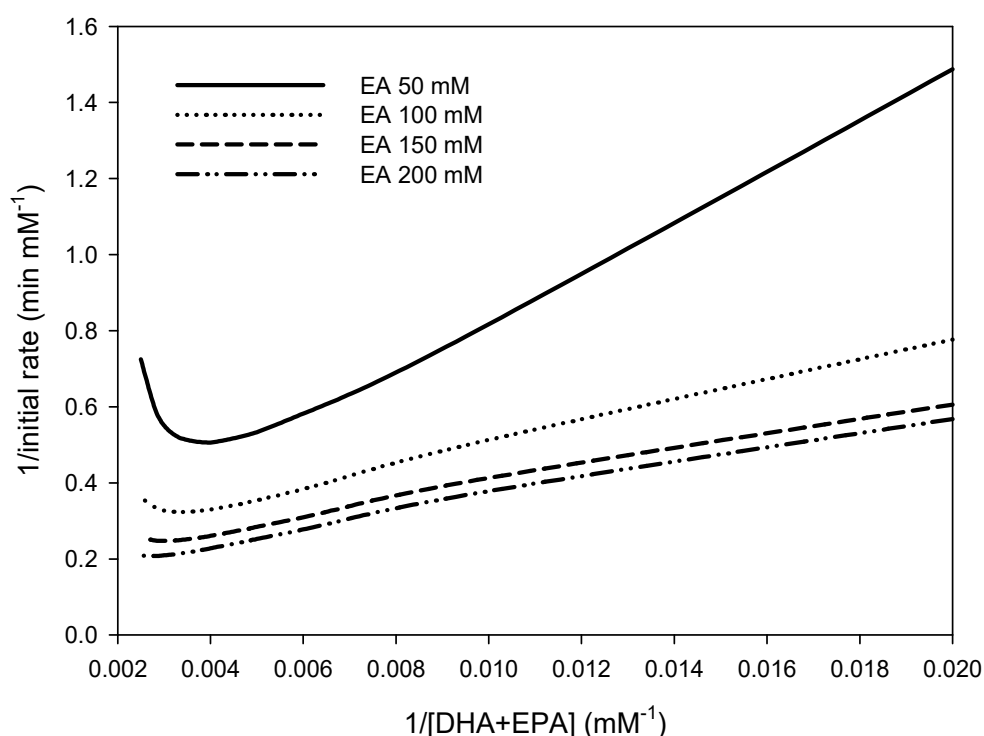


Figure 2. Lineweaver-Burk plot of reciprocal initial reaction rate vs. reciprocal concentrations of DHA+EPA concentrate at various EA concentrations during the synthesis of DHA+EPA ethyl ester via lipase-catalyzed acidolysis.

To determine kinetic constants, the initial rates obtained from RSM results were fitted to Equation (2) by non-linear regression analysis using the Polymath 6.0 program (Polymath Software, Willimantic, CT, USA). The fitness of the kinetic model was confirmed by a satisfactory value of the determination coefficient ($R^2 = 0.9$). The estimated kinetic constants are listed in Table 3. Based on the calculated kinetic constants, K_{mB} was found to be lower than K_{mA} , showing higher EA affinity towards immobilized lipase. These results agree with the ordered mechanism. Initially, EA binds to immobilized lipase (due to higher affinity) and forms an EA-enzyme complex (E-EA). DHA or EPA then combines with E-EA to form a ternary complex (E-EA-DHA or E-EA-EPA) and is further isomerized into a new complex (E-DHA ethyl ester-Acetic acid or E-EPA ethyl ester-Acetic acid). This ternary complex is broken down into acetic acid, while the binary complex subsequently releases DHA ethyl ester or EPA ethyl ester and enzyme. The ordered mechanism has also been proposed for lipase-catalyzed transesterification that uses vinyl

acetate as ester in the synthesis of geranyl acetate [58,59], *N*-(2-hydroxyphenyl) acetamide [60], and (*R*)-1-(pyridin-4-yl) ethyl acetate [61]. One of the most frequently reactions used to incorporate novel fatty acids into triacylglycerol is lipase-catalyzed acidolysis, several researches have been employed immobilized lipase as catalyst and no water is involved in the acidolysis reaction [62–64]. Kim and Hill Jr have been used both free and immobilized lipases to synthesize structured lipid containing pinolenic acid via lipase-catalyzed acidolysis, the use of immobilized lipase gives the higher degree of incorporation than use of free lipase [65]. This is due to the immobilization may alter the behavior in this reaction [66]. Besides, Verdasco-Martín et. al. have been reported the drying of substrate and immobilized enzyme on the hydrophobic supports are the key parameter to enhance the product yield and decrease the reaction time in the acidolysis reaction [67].

Table 3. Kinetic constants of lipase-catalyzed acidolysis in the synthesis of DHA+EPA ethyl ester.

Parameters	V_{max} (mM min ⁻¹)	K_{mA} (mM)	K_{mB} (mM)	K_{dA}
Values	14.33	416.97	155.96	49.72

2.3. Modelling of Lipase-Catalyzed Acidolysis Reaction

In this study, the kinetic model of the ordered mechanism was employed to simulate the performance of the batch reactor. The rate equation of the order mechanism described above in Equation (2) was integrated, giving rise to the following Equation (3) [53,68]:

$$kcat \frac{E_T t}{V} = [A]_0 X - K_{mA} \ln(1 - X) - K_{mB} \frac{[A]_0}{[B]_0} \ln(1 - X) + \frac{K_{dA} K_{mB}}{[B]_0} \left(\frac{1}{1 - X} - 1 \right) \quad (3)$$

where X is the degree of conversion, $kcat E_T$ is the maximum initial reaction rate (V_{max}), E_T is the total amount of enzyme, t is the time, and V is the liquid volume. The time curves were calculated from Equation (3) to predict the conversion of 50 mM DHA+EPA concentrate to DHA+EPA ethyl esters with different concentrations of EA. Figure 3 shows the comparison between the experimental results and the predicted curves, as calculated from Equation (3). A good fit between the experimental and predicted values was obtained, indicating that the proposed kinetic model is valid for this experiment.

2.4. Effect of DHA+EPA Concentration

Figure 4 shows the effects of varying concentrations of DHA+EPA concentrate on the conversion of DHA+EPA ethyl ester were investigated with a constant enzyme activity of 200 U, substrate ratio of 1:1 (DHA+EPA: EA), and reaction time of 300 min. After the reaction, the molar conversions were 93%, 94%, 89%, and 89% for DHA+EPA concentrate of 100 mM, 200 mM, 300 mM, and 400 mM, respectively. Conversion decreased slightly as concentration of DHA+EPA concentrate increased. Conversion at high concentrations of DHA+EPA concentrate (400 mM) was still 89%, indicating the lipase-catalyzed acidolysis of EA with DHA+EPA concentrate was very efficient. The reaction scheme is shown in Scheme 2, and the reaction product is easy to recover. After the reaction, the remaining reactant EA, acetic acid byproduct, and reaction solvent hexane are removed by a vacuum rotary evaporator in order to obtain the DHA+EPA ethyl ester. Lipase-catalyzed reactions for the synthesis of DHA-enriched esters have been widely investigated. Wang et al. reported on the modification of phosphatidylcholine with n-3 PUFA-rich ethyl esters by immobilized MAS1, via lipase-catalyzed transesterification that incorporated 43.55% n-3 PUFA into phosphatidylcholine after 72 h [69]. Zhang et al. used lipase-catalyzed ethanolysis of algal oil to synthesize 2-docosahexaenoylglycerol; product yields of 27–31% were obtained [70]. Bhandari et al. obtained 76.2% esterification after 24 h from the selective esterification of tuna-FFA with butanol using *Rhizopus oryzae* lipase [71]. This study shows the advantages of lipase-catalyzed acidolysis. Not only is DHA+EPA ethyl ester synthesized efficiently, the product can also be easily recovered.

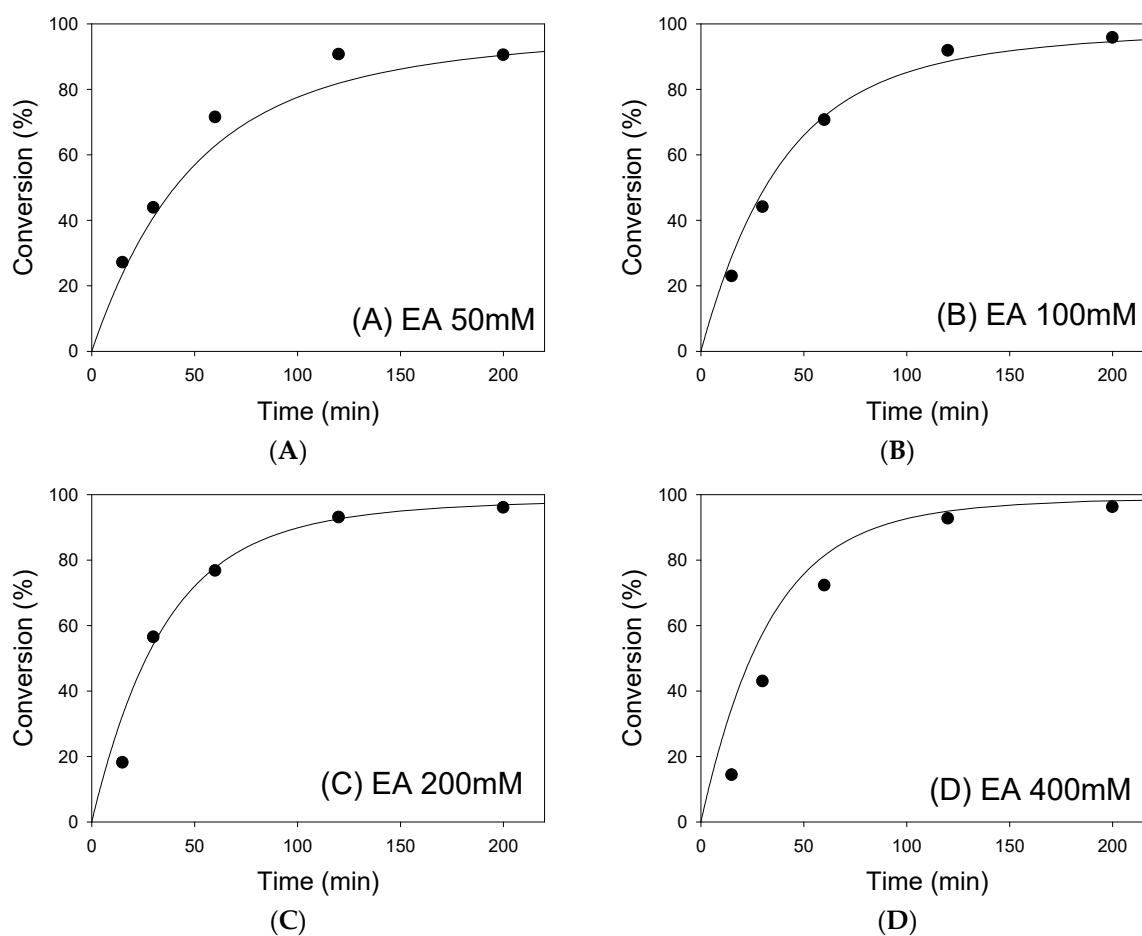


Figure 3. Comparison of experimental results and the simulated conversions obtained from the integrated rate equation (Equation (3)) using 50 mM DHA+EPA concentrate with (A) 50, (B) 100, (C) 200, and (D) 400 mM EA. Points are experimental data and lines are predicted from integrated rate equation (Equation (3)).

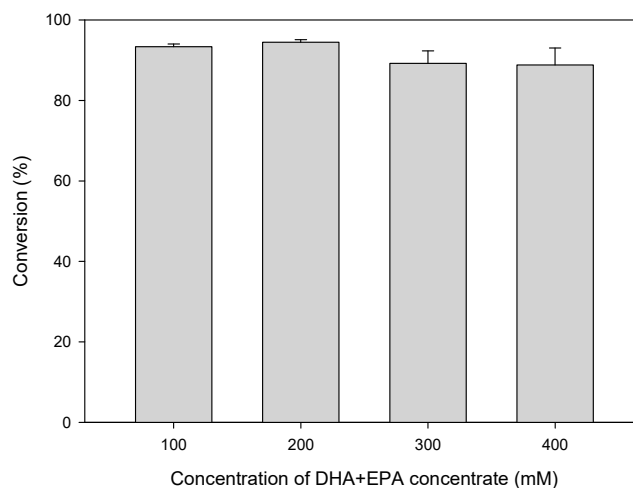


Figure 4. Effect of concentration of DHA+EPA concentrate on the conversion of DHA+EPA ethyl ester at a substrate ratio of 1:1 (DHA+EPA: EA), temperature of 60 °C, and enzyme activity of 200 U.

3. Materials and Methods

3.1. Materials

Cobia livers were collected from Cobiahome Inc. (Pingtung, Taiwan). Novozym[®] 435 (10,000 U/g; propyl laurate units (PLU)), lipase from *Candida antarctica* B (EC3.1.1.3) immobilized on a macroporous acrylic resin was obtained from Novo Nordisk Bioindustrials Inc. (Copenhagen, Denmark). Ethyl acetate (99.8%) was produced from Merck (Darmstadt, Germany). Fatty acid methyl ester standards (Supelco 37 Component FAME Mix, Catalog No. 47885) and BF₃-methanol reagent (14% BF₃ in CH₃OH, *w/v*) were purchased from Sigma-Aldrich (St. Louis, MO, USA). *cis*-4,7,10,13,16,19-Docosahexaenoic acid used for analysis was purchased from Acros (NJ, USA). *cis*-5,8,11,14,17-Eicosapentaenoic acid used for analysis was purchased from TCI Co., LTD. (Tokyo, Japan). Unless otherwise specified, all reagents and chemicals used in this study were of analytical grade.

3.2. Cobia Liver Oil Extraction and Preparation of DHA+EPA Concentrate

Cobia liver oil was extracted using the homogenization method, as described elsewhere [72]. The extracted crude oil was saponified to obtain free fatty acids (FFAs), as described by Chen and Ju [17]. The DHA+EPA concentrate was prepared from the FFAs by using the acetone fractionation of fatty acid salts method, as described elsewhere [52]. Briefly, 50 g FFAs was mixed with 695 mL acetone and preheated at 30 °C for 30 min. This was followed by the addition of 8.5 mL 15 N NaOH aqueous solution. The solution was reacted for 90 min with a magnetic stirrer at 550 rpm. A Buchner funnel were used to separate the solid and liquid phases. 400 mL of distilled water was added to the filtrate, and pH was adjusted to 1 by adding 12 N hydrochloric acid for recovering FFAs from the corresponding sodium salts, followed by extraction with 250 mL hexane for 20 min. The hexane layer was collected using a separating funnel, and the hexane was removed by vacuum rotary evaporator at 70 °C to recover the DHA+EPA concentrate. The fatty acid profiles of the DHA+EPA concentrate were analyzed by the GC method, as described elsewhere [72]. The fatty acid profile of DHA+EPA concentrate was 54.4% DHA, 16.8% EPA, 7.0% docosadienoic acid, 14.2% oleic acid, 0.8% linoleic acid, 0.5% linolenic acid, 3.1% palmitoleic acid, 2.7% palmitic acid and 0.5% myristic acid.

3.3. Experimental Design for Determining the Kinetic Constants

Lipase-catalyzed acidolysis of EA with DHA+EPA concentrate was investigated by RSM in order to evaluate the effect of substrate concentration on the reaction rate. A five-level–two-factor central composite design was employed to determine the kinetic constants. Table 1 shows the substrate concentrations (x_i), levels, and experimental design in terms of coded or uncoded. The acidolysis reactions were performed at 60 °C in *n*-hexane for the initial rate measurements. 20 mg immobilized lipase Novozym[®] 435 was added to 3 mL of the reaction mixture, containing various amounts of DHA+EPA concentrate and EA, for a 20 min incubation period. All reactions were done in duplicate. After the reaction, liquid samples were withdrawn from the reaction mixture to determine the produced DHA+EPA ethyl ester using HPLC. Initial reaction rates are expressed as produced μmol of DHA+EPA ethyl ester per unit of enzyme for 1 min ($\mu\text{mol min}^{-1} \text{U}^{-1}$). The polymath 6.0 (Polymath Software, Willimantic, CT, USA) was used to calculate kinetic constants by nonlinear regression using, based on 898 data points obtained from the RSM results.

3.4. Lipase-Catalyzed Synthesis of DHA+EPA Ethyl Ester

Lipase-catalyzed acidolysis was carried out in a capped glass tube (diameter 1.5 cm) with different concentrations of DHA+EPA concentrate and EA, supplemented with *n*-hexane to bring the total volume to 3 mL. 20 mg immobilized lipase Novozym[®] 435 was then added to initiate the reaction. The reaction mixture was agitated in an orbital shaking bath (150 rpm) at 60 °C. All reactions were

done in duplicate. Samples were withdrawn from the reaction mixture at different times and analyzed by HPLC. The amount of DHA+EPA concentrate added was calculated by the following equation:

$$DHA + EPA \text{ concentrate added}(\mu\text{L}) = DHA + EPA \text{ concentration}(mM) \times 0.003 \times 312 \div 0.864 \quad (4)$$

where 0.003 is the total reaction volume, 312 is the average molecular weight of DHA+EPA concentrate, and 0.864 is the specific gravity of DHA+EPA concentrate.

3.5. Analytical Methods

The samples were analyzed by Hitachi HPLC system (Hitachi, Tokyo, Japan), consisting of a pump (L-23130), and a UV/VIS detector (L-2420), and Inertsil ODS-3 column (5 μM , 250 mm \times 4.6 mm). The mobile phase were deionized water and methanol containing 0.1% acetic acid. The gradient elution was started from 80% to 100% methanol for 10 min, followed by elution at 100% methanol for 20 min. The flow rate and UV detector were set at 1.0 mL min^{-1} and wavelength of 303 nm, respectively. The conversion yield % was calculated from the peak areas of the substrate (DHA+EPA) and product (DHA+EPA ethyl ester).

3.6. Statistical Analysis

Experimental data (Table 1) were analyzed by the response surface regression (RSREG) procedure of SAS (SAS Institute, Cary, NC) to fit the following second-order polynomial equation:

$$Y = \beta_k + \sum \beta_{ki} X_i + \sum \beta_{kii} X_i^2 + \sum \sum \beta_{kij} X_i X_j \quad (5)$$

where Y is the response, β_{k0} , β_{ki} , β_{kii} and β_{kij} are the constant coefficients, and X_i and X_j are the uncoded independent variables.

4. Conclusions

Lipase-catalyzed acidolysis of EA with DHA+EPA concentrate was first reported for synthesizing DHA+EPA ethyl esters. A 5-level-2-factor central composite design was used to evaluate the initial rate in order to determine the reaction mechanism. Based on the slopes of Lineweaver-Burk plots, the reaction followed the ordered mechanism. The initial rate data calculated from the RSM results was also a good fit to the ordered mechanism kinetic model. The proposed kinetic model integrated with a batch mole balance equation could be used to predict experimental conversions. There was a good correlation between the experimental conversion data and the predicted data from the integrated equation. The high conversion of DHA+EPA ethyl ester (94%) was obtained at the DHA+EPA concentrate of 200 mM, enzyme activity of 200 U, substrate ratio of 1:1 (DHA+EPA: EA), and reaction time of 300 min. Esterification of DHA or EPA concentrate with EA via acidolysis seems to be a more suitable strategy than with ethanol, as the data presented here confirms that lipase-catalyzed acidolysis is a potential reaction pathway for ester synthesis.

Author Contributions: Conceptualization, C.-H.K. and C.-J.S.; software, C.-H.K.; investigation, C.-H.K.; resources, C.-Y.H., C.-L.L., W.-C.K. and S.-L.H.; writing—original draft preparation, C.-H.K.; writing—review and editing, C.-H.K. and C.-J.S. All authors have read and agree to the published version of the manuscript.

Funding: This work was supported by research funding grants provided by the Ministry of Science and Technology of Taiwan (MOST 104-2218-E-022-001-MY2 and MOST 108-2221-E-992-048)

Conflicts of Interest: The authors declare no conflict of interest.

References

1. Finco, A.M.D.O.; Mamani, L.D.G.; Carvalho, J.C.D.; de Melo Pereira, G.V.; Thomaz-Soccol, V.; Soccol, C.R. Technological trends and market perspectives for production of microbial oils rich in omega-3. *Crit. Rev. Biotechnol.* **2017**, *37*, 656–671. [[CrossRef](#)]

2. Liu, S.-H.; Chiu, C.-Y.; Wang, L.-P.; Chiang, M.-T. Omega-3 fatty acids-enriched fish oil activates AMPK/PGC-1 α signaling and prevents obesity-related skeletal muscle wasting. *Mar. Drugs* **2019**, *17*, 380. [[CrossRef](#)]
3. Minihane, A. Impact of genotype on EPA and DHA status and responsiveness to increased intakes. *Nutrients* **2016**, *8*, 123. [[CrossRef](#)]
4. Haug, I.J.; Sagmo, L.B.; Zeiss, D.; Olsen, I.C.; Draget, K.I.; Seternes, T. Bioavailability of EPA and DHA delivered by gelled emulsions and soft gel capsules. *Eur. J. Lipid Sci. Technol.* **2011**, *113*, 137–145. [[CrossRef](#)]
5. Yamazaki, T.; Li, D.; Ikaga, R. Effective food ingredients for fatty liver: Soy protein β -conglycinin and fish oil. *Int. J. Mol. Sci.* **2018**, *19*, 4107. [[CrossRef](#)]
6. Liu, X.; Cui, J.; Li, Z.; Xu, J.; Wang, J.; Xue, C.; Wang, Y. Comparative study of DHA-enriched phospholipids and EPA-enriched phospholipids on metabolic disorders in diet-induced-obese C57BL/6J mice. *Eur. J. Lipid Sci. Technol.* **2014**, *116*, 255–265. [[CrossRef](#)]
7. Stoodley, I.; Garg, M.; Scott, H.; Macdonald-Wicks, L.; Berthon, B.; Wood, L. Higher omega-3 index is associated with better asthma control and lower medication dose: A cross-sectional study. *Nutrients* **2020**, *12*, 74. [[CrossRef](#)]
8. Jeong, Y.K.; Kim, H. A mini-review on the effect of docosahexaenoic acid (DHA) on cerulein-induced and hypertriglyceridemic acute pancreatitis. *Int. J. Mol. Sci.* **2017**, *18*, 2239. [[CrossRef](#)]
9. Mohanty, B.P.; Ganguly, S.; Mahanty, A.; Sankar, T.; Anandan, R.; Chakraborty, K.; Paul, B.; Sarma, D.; Syama Dayal, J.; Venkateshwarlu, G. DHA and EPA content and fatty acid profile of 39 food fishes from India. *Biomed Res. Int.* **2016**, 4027437. [[CrossRef](#)]
10. Mu, H.; Zhang, H.; Li, Y.; Zhang, Y.; Wang, X.; Jin, Q.; Wang, X. Enrichment of DPAn-6 and DHA from *Schizochytrium sp.* oil by low-temperature solvent crystallization. *Ind. Eng. Chem. Res.* **2016**, *55*, 737–746. [[CrossRef](#)]
11. Dovale-Rosabal, G.; Rodríguez, A.; Contreras, E.; Ortiz-Viedma, J.; Muñoz, M.; Trigo, M.; Aubourg, S.P.; Espinosa, A. Concentration of EPA and DHA from refined salmon oil by optimizing the urea–fatty acid adduction reaction conditions using response surface methodology. *Molecules* **2019**, *24*, 1642. [[CrossRef](#)]
12. Vázquez, L.; Prados, I.M.; Reglero, G.; Torres, C.F. Identification and quantification of ethyl carbamate occurring in urea complexation processes commonly utilized for polyunsaturated fatty acid concentration. *Food Chem.* **2017**, *229*, 28–34. [[CrossRef](#)]
13. Solaesa, Á.G.; Sanz, M.T.; Falkeborg, M.; Beltrán, S.; Guo, Z. Production and concentration of monoacylglycerols rich in omega-3 polyunsaturated fatty acids by enzymatic glycerolysis and molecular distillation. *Food Chem.* **2016**, *190*, 960–967. [[CrossRef](#)]
14. Montañés, F.; Tallon, S. Supercritical fluid chromatography as a technique to fractionate high-valued compounds from lipids. *Separations* **2018**, *5*, 38. [[CrossRef](#)]
15. Jiao, G.; Hui, J.; Burton, I.; Thibault, M.-H.; Pelletier, C.; Boudreau, J.; Tchoukanova, N.; Subramanian, B.; Djaoed, Y.; Ewart, S. Characterization of shrimp oil from *Pandalus borealis* by high performance liquid chromatography and high resolution mass spectrometry. *Mar. Drugs* **2015**, *13*, 3849–3876. [[CrossRef](#)]
16. Rincón Cervera, M.Á.; Venegas, E.; Ramos Bueno, R.P.; Suárez Medina, M.D.; Guil Guerrero, J.L. Docosahexaenoic acid purification from fish processing industry by-products. *Eur. J. Lipid Sci. Technol.* **2015**, *117*, 724–729. [[CrossRef](#)]
17. Chen, T.-C.; Ju, Y.-H. Enrichment of eicosapentaenoic acid and docosahexaenoic acid in saponified menhaden oil. *J. Am. Oil Chem. Soc.* **2000**, *77*, 425–428. [[CrossRef](#)]
18. Castejón, N.; Señoráns, F.J. Strategies for enzymatic synthesis of omega-3 structured triacylglycerols from *Camelina sativa* oil enriched in EPA and DHA. *Eur. J. Lipid Sci. Technol.* **2019**, *121*, 1800412. [[CrossRef](#)]
19. Valverde, L.M.; Moreno, P.A.G.; Callejón, M.J.J.; Cerdán, L.E.; Medina, A.R. Concentration of eicosapentaenoic acid (EPA) by selective alcoholysis catalyzed by lipases. *Eur. J. Lipid Sci. Technol.* **2013**, *115*, 990–1004. [[CrossRef](#)]
20. Morais Júnior, W.G.; Fernández-Lorente, G.; Guisán, J.M.; Ribeiro, E.J.; De Resende, M.M.; Costa Pessela, B. Production of omega-3 polyunsaturated fatty acids through hydrolysis of fish oil by *Candida rugosa* lipase immobilized and stabilized on different supports. *Biocatal. Biotransform.* **2017**, *35*, 63–73. [[CrossRef](#)]
21. Miyashita, K.; Takagi, T. Study on the oxidative rate and prooxidant activity of free fatty acids. *J. Am. Oil Chem. Soc.* **1986**, *63*, 1380–1384. [[CrossRef](#)]

22. Hills, G. Industrial use of lipases to produce fatty acid esters. *Eur. J. Lipid Sci. Technol.* **2003**, *105*, 601–607. [CrossRef]
23. Verma, M.L.; Rao, N.M.; Tsuzuki, T.; Barrow, C.J.; Puri, M. Suitability of recombinant lipase immobilised on functionalised magnetic nanoparticles for fish oil hydrolysis. *Catalysts* **2019**, *9*, 420. [CrossRef]
24. Souza, L.T.d.A.; Moreno-Perez, S.; Fernández Lorente, G.; Cipolatti, E.P.; De Oliveira, D.; Resende, R.R.; Pessela, B.C. Immobilization of *moniliella spathulata* r251270 lipase on ionic, hydrophobic and covalent supports: Functional properties and hydrolysis of sardine oil. *Molecules* **2017**, *22*, 1508. [CrossRef]
25. Huang, S.-M.; Li, H.-J.; Liu, Y.-C.; Kuo, C.-H.; Shieh, C.-J. An efficient approach for lipase-catalyzed synthesis of retinyl laurate nutraceutical by combining ultrasound assistance and artificial neural network optimization. *Molecules* **2017**, *22*, 1972. [CrossRef]
26. Huang, S.-M.; Hung, T.-H.; Liu, Y.-C.; Kuo, C.-H.; Shieh, C.-J. Green synthesis of ultraviolet absorber 2-ethylhexyl salicylate: Experimental design and artificial neural network modeling. *Catalysts* **2017**, *7*, 342. [CrossRef]
27. Mendoza-Ortiz, P.A.; Gama, R.S.; Gómez, O.C.; Luiz, J.H.; Fernandez-Lafuente, R.; Cren, E.C.; Mendes, A.A. Sustainable enzymatic synthesis of a solketal ester—process optimization and evaluation of its antimicrobial activity. *Catalysts* **2020**, *10*, 218. [CrossRef]
28. Yang, H.; Zhang, W. Surfactant imprinting hyperactivated immobilized lipase as efficient biocatalyst for biodiesel production from waste cooking oil. *Catalysts* **2019**, *9*, 914. [CrossRef]
29. Mateo, C.; Palomo, J.M.; Fernandez-Lorente, G.; Guisan, J.M.; Fernandez-Lafuente, R. Improvement of enzyme activity, stability and selectivity via immobilization techniques. *Enzym. Microb. Technol.* **2007**, *40*, 1451–1463. [CrossRef]
30. Derewenda, U.; Brzozowski, A.M.; Lawson, D.M.; Derewenda, Z.S. Catalysis at the interface: The anatomy of a conformational change in a triglyceride lipase. *Biochemistry* **1992**, *31*, 1532–1541. [CrossRef]
31. Manoel, E.A.; dos Santos, J.C.; Freire, D.M.; Rueda, N.; Fernandez-Lafuente, R. Immobilization of lipases on hydrophobic supports involves the open form of the enzyme. *Enzym. Microb. Technol.* **2015**, *71*, 53–57. [CrossRef] [PubMed]
32. Fernandez-Lafuente, R.; Armisen, P.; Sabuquillo, P.; Fernández-Lorente, G.; Guisán, J.M. Immobilization of lipases by selective adsorption on hydrophobic supports. *Chem. Phys. Lipids* **1998**, *93*, 185–197. [CrossRef]
33. Cabrera, Z.; Fernandez-Lorente, G.; Fernandez-Lafuente, R.; Palomo, J.M.; Guisan, J.M. Novozym 435 displays very different selectivity compared to lipase from *Candida antarctica* B adsorbed on other hydrophobic supports. *J. Mol. Catal. B Enzym.* **2009**, *57*, 171–176. [CrossRef]
34. Chen, G.J.; Kuo, C.H.; Chen, C.I.; Yu, C.C.; Shieh, C.J.; Liu, Y.C. Effect of membranes with various hydrophobic/hydrophilic properties on lipase immobilized activity and stability. *J. Biosci. Bioeng.* **2012**, *113*, 166–172. [CrossRef]
35. Ortiz, C.; Ferreira, M.L.; Barbosa, O.; dos Santos, J.C.; Rodrigues, R.C.; Berenguer-Murcia, Á.; Briand, L.E.; Fernandez-Lafuente, R. Novozym 435: The “perfect” lipase immobilized biocatalyst? *Catal. Sci. Technol.* **2019**, *9*, 2380–2420. [CrossRef]
36. Shimada, Y.; Watanabe, Y.; Sugihara, A.; Baba, T.; Ooguri, T.; Moriyama, S.; Terai, T.; Tominaga, Y. Ethyl esterification of docosahexaenoic acid in an organic solvent-free system with immobilized *Candida antarctica* lipase. *J. Biosci. Bioeng.* **2001**, *92*, 19–23. [CrossRef]
37. Poisson, L.; Ergon, F. Docosahexaenoic acid ethyl esters from *Isochrysis galbana*. *J. Biotechnol.* **2001**, *91*, 75–81. [CrossRef]
38. Bhandari, K.; Chaurasia, S.; Dalai, A. Lipase-catalyzed esterification of docosahexaenoic acid-rich fatty acids with glycerol. *Chem. Eng. Commun.* **2015**, *202*, 920–926. [CrossRef]
39. Roby, M.H.H. Synthesis and characterization of phenolic lipids. In *Phenolic Compounds-Natural Sources, Importance and Applications*; IntechOpen: London, UK, 2017; Available online: <https://www.intechopen.com/books/phenolic-compounds-natural-sources-importance-and-applications/synthesis-and-characterization-of-phenolic-lipids> (accessed on 18 May 2020).
40. Kuo, C.H.; Ju, H.Y.; Chu, S.W.; Chen, J.H.; Chang, C.M.J.; Liu, Y.C.; Shieh, C.J. Optimization of lipase-catalyzed synthesis of cetyl octanoate in supercritical carbon dioxide. *J. Am. Oil Chem. Soc.* **2012**, *89*, 103–110. [CrossRef]
41. Chen, H.C.; Kuo, C.H.; Twu, Y.K.; Chen, J.H.; Chang, C.M.J.; Liu, Y.C.; Shieh, C.J. A continuous ultrasound-assisted packed-bed bioreactor for the lipase-catalyzed synthesis of caffeic acid phenethyl ester. *J. Chem. Technol. Biotechnol.* **2011**, *86*, 1289–1294. [CrossRef]

42. Kuo, C.H.; Chiang, S.H.; Ju, H.Y.; Chen, Y.M.; Liao, M.Y.; Liu, Y.C.; Shieh, C.J. Enzymatic synthesis of rose aromatic ester (2-phenylethyl acetate) by lipase. *J. Sci. Food Agric.* **2012**, *92*, 2141–2147. [[CrossRef](#)] [[PubMed](#)]
43. Yankah, V.V.; Akoh, C.C. Lipase-catalyzed acidolysis of tristearin with oleic or caprylic acids to produce structured lipids. *J. Am. Oil Chem. Soc.* **2000**, *77*, 495–500. [[CrossRef](#)]
44. Mitra, K.; Kim, S.A.; Lee, J.H.; Choi, S.W.; Lee, K.T. Production and characterization of α -linolenic acid enriched structured lipids from lipase-catalyzed interesterification. *Food Sci. Biotechnol.* **2010**, *19*, 57–62. [[CrossRef](#)]
45. Rychlicka, M.; Niezgoda, N.; Gliszczynska, A. Lipase-catalyzed acidolysis of egg-yolk phosphatidylcholine with citronellic acid. New insight into synthesis of isoprenoid-phospholipids. *Molecules* **2018**, *23*, 314. [[CrossRef](#)]
46. Chojnacka, A.; Gładkowski, W. Production of structured phosphatidylcholine with high content of myristic acid by lipase-catalyzed acidolysis and interesterification. *Catalysts* **2018**, *8*, 281. [[CrossRef](#)]
47. Yue, C.; Ben, H.; Wang, J.; Li, T.; Yu, G. Ultrasonic pretreatment in synthesis of caprylic-rich structured lipids by lipase-catalyzed acidolysis of corn oil in organic system and its physicochemical properties. *Foods* **2019**, *8*, 566. [[CrossRef](#)]
48. Arıkaya, A.; Ünlü, A.E.; Takaç, S. Use of deep eutectic solvents in the enzyme catalysed production of ethyl lactate. *Process Biochem.* **2019**, *84*, 53–59. [[CrossRef](#)]
49. Cavallaro, V.; Tonetto, G.; Ferreira, M.L. Optimization of the enzymatic synthesis of pentyl oleate with lipase immobilized onto novel structured support. *Fermentation* **2019**, *5*, 48. [[CrossRef](#)]
50. Yadav, G.D.; Kamble, M.P. A green process for synthesis of geraniol esters by immobilized lipase from *Candida antarctica* B fraction in non-aqueous reaction media: Optimization and kinetic modeling. *Int. J. Chem. React. Eng.* **2018**, *16*. [[CrossRef](#)]
51. Jaiswal, K.S.; Rathod, V.K. Acoustic cavitation promoted lipase catalysed synthesis of isobutyl propionate in solvent free system: Optimization and kinetic studies. *Ultrason. Sonochem.* **2018**, *40*, 727–735. [[CrossRef](#)]
52. Kuo, C.H.; Huang, C.Y.; Chen, J.W.; Wang, H.M.D.; Shieh, C.J. Concentration of docosahexaenoic and eicosapentaenoic acid from cobia liver oil by acetone fractionation of fatty acid salts. *Appl. Biochem. Biotechnol.* **2020**. [[CrossRef](#)] [[PubMed](#)]
53. Oliveira, A.; Rosa, M.; Aires-Barros, M.; Cabral, J. Enzymatic esterification of ethanol and oleic acid—A kinetic study. *J. Mol. Catal. B Enzym.* **2001**, *11*, 999–1005. [[CrossRef](#)]
54. Parikh, D.T.; Lanjekar, K.J.; Rathod, V.K. Kinetics and thermodynamics of lipase catalysed synthesis of propyl caprate. *Biotechnol. Lett.* **2019**, *41*, 1163–1175. [[CrossRef](#)] [[PubMed](#)]
55. Krishna, S.H.; Karanth, N. Lipase-catalyzed synthesis of isoamyl butyrate: A kinetic study. *Biochim. Biophys. Acta-Protein Struct. Mol. Enzym.* **2001**, *1547*, 262–267. [[CrossRef](#)]
56. Daneshfar, A.; Ghaziaskar, H.; Shiri, L.; Manafi, M.; Nikorazm, M.; Abassi, S. Synthesis of 2-ethylhexyl-2-ethylhexanoate catalyzed by immobilized lipase in n-hexane: A kinetic study. *Biochem. Eng. J.* **2007**, *37*, 279–284. [[CrossRef](#)]
57. Alberty, R.A. The relationship between Michaelis constants, maximum velocities and the equilibrium constant for an enzyme-catalyzed reaction. *J. Am. Chem. Soc.* **1953**, *75*, 1928–1932. [[CrossRef](#)]
58. Badgujar, K.C.; Bhanage, B.M. Synthesis of geranyl acetate in non-aqueous media using immobilized *Pseudomonas cepacia* lipase on biodegradable polymer film: Kinetic modelling and chain length effect study. *Process Biochem.* **2014**, *49*, 1304–1313. [[CrossRef](#)]
59. Patel, V.; Shah, C.; Deshpande, M.; Madamwar, D. Zinc oxide nanoparticles supported lipase immobilization for biotransformation in organic solvents: A facile synthesis of geranyl acetate, effect of operative variables and kinetic study. *Appl. Biochem. Biotechnol.* **2016**, *178*, 1630–1651. [[CrossRef](#)]
60. Magadum, D.B.; Yadav, G.D. Chemoselective acetylation of 2-aminophenol using immobilized lipase: Process optimization, mechanism, and kinetics. *ACS Omega* **2018**, *3*, 18528–18534. [[CrossRef](#)]
61. Magadum, D.B.; Yadav, G.D. One-pot synthesis of (R)-1-(pyridin-4-yl) ethyl acetate using tandem catalyst prepared by co-immobilization of palladium and lipase on mesoporous foam: Optimization and kinetic modeling. *Chirality* **2017**, *29*, 811–823. [[CrossRef](#)]
62. Wang, J.; Shahidi, F. Acidolysis of p-coumaric acid with omega-3 oils and antioxidant activity of phenolipid products in in vitro and biological model systems. *J. Agric. Food Chem.* **2014**, *62*, 454–461. [[CrossRef](#)] [[PubMed](#)]

63. Yanık, D.K.; Keskin, H.; Fadiloğlu, S.; Göğüş, F. Acidolysis reaction of terebinth fruit oil with palmitic and caprylic acids to produce low caloric spreadable structured lipid. *J. Am. Oil Chem. Soc.* **2013**, *90*, 999–1009. [[CrossRef](#)]
64. Ifeduba, E.A.; Akoh, C.C. Modification of stearidonic acid soybean oil by immobilized *Rhizomucor miehei* lipase to incorporate caprylic acid. *J. Am. Oil Chem. Soc.* **2014**, *91*, 953–965. [[CrossRef](#)]
65. Kim, I.H.; Hill, C.G., Jr. Lipase-catalyzed acidolysis of menhaden oil with pinolenic acid. *J. Am. Oil Chem. Soc.* **2006**, *83*, 109–115. [[CrossRef](#)]
66. Rodrigues, R.C.; Ortiz, C.; Berenguer-Murcia, Á.; Torres, R.; Fernández-Lafuente, R. Modifying enzyme activity and selectivity by immobilization. *Chem. Soc. Rev.* **2013**, *42*, 6290–6307. [[CrossRef](#)]
67. Verdasco-Martín, C.M.; Corchado-Lopo, C.; Fernández-Lafuente, R.; Otero, C. Rapid and high yield production of phospholipids enriched in CLA via acidolysis: The critical role of the enzyme immobilization protocol. *Food Chem.* **2019**, *296*, 123–131. [[CrossRef](#)]
68. Kuo, C.-H.; Chen, G.-J.; Chen, C.-I.; Liu, Y.-C.; Shieh, C.-J. Kinetics and optimization of lipase-catalyzed synthesis of rose fragrance 2-phenylethyl acetate through transesterification. *Process Biochem.* **2014**, *49*, 437–444. [[CrossRef](#)]
69. Wang, X.; Qin, X.; Li, X.; Zhao, Z.; Yang, B.; Wang, Y. Insight into the modification of phosphatidylcholine with n-3 polyunsaturated fatty acids-rich ethyl esters by immobilized MAS1 lipase. *Molecules* **2019**, *24*, 3528. [[CrossRef](#)]
70. Zhang, Y.; Wang, X.; Zou, S.; Xie, D.; Jin, Q.; Wang, X. Synthesis of 2-docosahexaenoylglycerol by enzymatic ethanolysis. *Bioresour. Technol.* **2018**, *251*, 334–340. [[CrossRef](#)]
71. Bhandari, K.; Chaurasia, S.; Dalai, A.; Gupta, A. Purification of free DHA by selective esterification of fatty acids from tuna oil catalyzed by *Rhizopus oryzae* lipase. *J. Am. Oil Chem. Soc.* **2013**, *90*, 1637–1644. [[CrossRef](#)]
72. Kuo, C.H.; Liao, H.Z.; Wang, Y.H.; Wang, H.M.D.; Shieh, C.J.; Tseng, C.Y. Highly efficient extraction of EPA/DHA-enriched oil from cobia liver using homogenization plus sonication. *Eur. J. Lipid Sci. Technol.* **2017**, *119*, 1600466. [[CrossRef](#)]



© 2020 by the authors. Licensee MDPI, Basel, Switzerland. This article is an open access article distributed under the terms and conditions of the Creative Commons Attribution (CC BY) license (<http://creativecommons.org/licenses/by/4.0/>).